

Simulated Meson Decays

Drew Silcock

Saturday 1st February, 2014

1 Introduction

The aim of this project is to examine the product particles of various meson decays, in particular B , D and $\psi(3770)$ decays. To this end, the invariant mass distributions of three decay chains were examined:

1. Two body $\psi(3770) \rightarrow D^0 \bar{D}^0$,
2. Three body $B^+ \rightarrow D^0 \bar{D}^0 K^+$, and
3. Four body $D^0 \rightarrow K^+ K^- K^- \pi^+$

In addition, the decay angles between the resulting particles in the lab frame were examined for the following decays:

1. $\psi(3770) \rightarrow D^0 \bar{D}^0$ and
2. $B \rightarrow \{\psi(3770) \rightarrow D^0 \bar{D}^0\} K$

2 Background

2.1 Purpose

The $\psi(3770)$ decays are of particular interest because the resultant D^0 and \bar{D}^0 are produced in a quantum correlated state. This allows for better access to D^0 phase information introduced by the strong force. This in turn is critical information in the accurate measurement of CP violation in beauty decays (e.g. $B \rightarrow DK$), which is a large part of the University of Bristol's LHCb programme. These $\psi(3770)$ decays can also be used to measure symmetry violations in the **charm** system.

CP violation contributes to the matter antimatter asymmetry that we see today, i.e. why the universe is full of matter and not antimatter. At present the amount of observed CP violation cannot

account for the extent of matter-antimatter asymmetry present. Analysis of the CP violation of both the beauty and charm decays involved with the $\psi(3770)$ decays could both lead to a better explanation of this matter-antimatter asymmetry, or to the discovery of New Physics.

2.2 ROOT Framework

The ROOT C++ framework and libraries were used for toy Monte Carlo (MC) decays and to analyse the results find the invariant mass distributions and decay angles in both the centre of mass frame and the laboratory frame. In particular the `GetDecay()::TGenPhaseSpace`, `M()::TLorentzVector` and `Angle()::TLorentzVector` methods were used to generate toy MC decays, get the invariant mass of a 4-vector and get the angle between two 4-vectors respectively.

3 Invariant Mass Distributions

Here the distribution of the invariant masses of the product particle of each decay chain were plotted and examined.

3.1 Two body $\psi(3770) \rightarrow D^0 \bar{D}^0$ decay

The plot of the invariant mass distribution of the $D^0 \bar{D}^0$, showing in Figure 1, matches exactly with the mass of the parent $\psi(3770)$ particle¹, which is exactly as would be expected for a two body decay:

¹Mass of $\psi(3770) = 3773.15 \pm 0.33$ MeV [1]

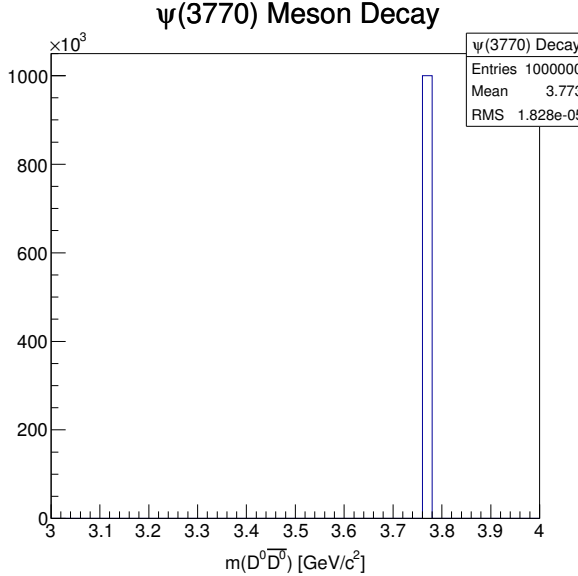


Figure 1: The invariant mass distribution of the $D^0\bar{D}^0$ corresponds exactly to the mass of the parent $\psi(3770)$.

3.2 Three body $B^+ \rightarrow D^0\bar{D}^0K^+$ decay

For the three body decay, the invariant mass distributions produces a 3-dimensional plot of the invariant mass combinations. These weighted distributions are shown below in Figures 2 and 3.

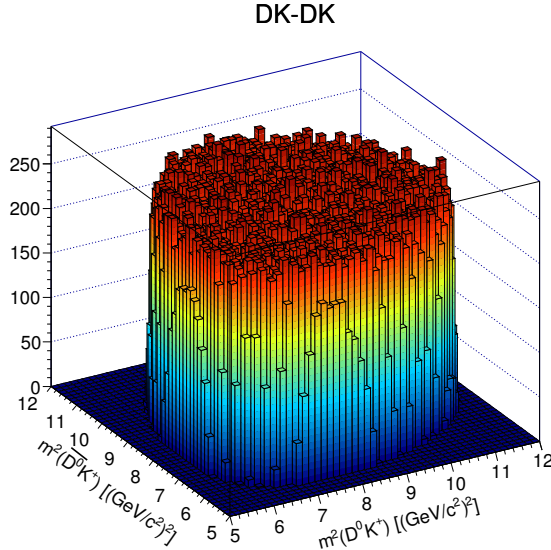


Figure 2: 3D plot showing the invariant mass distribution of D^0K^+ against \bar{D}^0K^+ . Note that the top of the distribution is roughly flat.

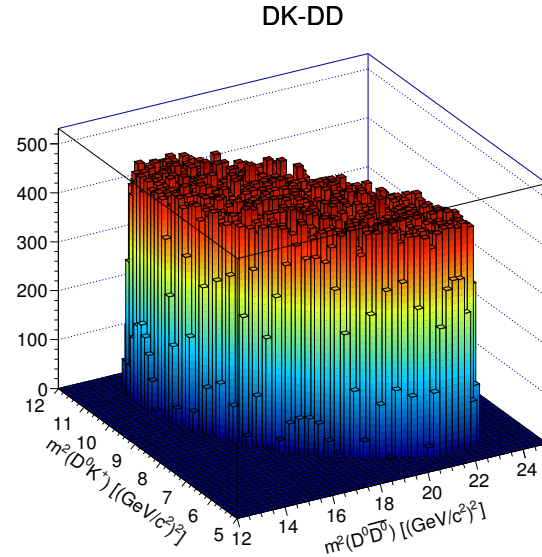


Figure 3: 3D plot showing the invariant mass distribution of D^0K^+ against $D^0\bar{D}^0$. Note that the top of this distribution is also roughly flat.

Three body decay has a two-dimensional phase space, so these data are best visualised as 3-dimensional density plots of the invariant mass distributions of two of the three combinations of the particles. Note that all of the essential information about the decay is contained in a single plot and the others can be derived from the one plot due to momentum conservation laws.

This simulation does not take into account intermediate resonances, which have the effect of altering the topology of the top of the plot so that it is no longer roughly flat-topped. One such resonance, which will be discussed in Section 4.2, is of particular interest.

3.3 Four body $D^0 \rightarrow K^+K^-K^-\pi^+$ decay

The four body decay produces a five dimensional phase space, which is projected onto various axes so that they can be easily analysed and understood.

The following projected plots were produced:

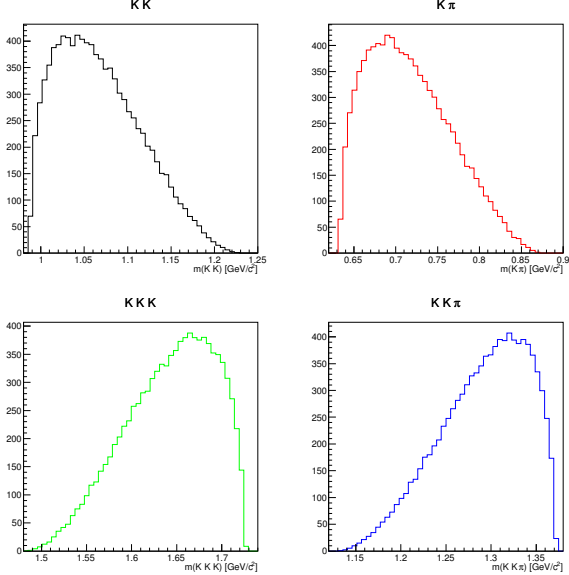


Figure 4: The projected plots of various invariant mass combinations for the four body decay $D^0 \rightarrow K^+ K^- K^- \pi^+$

Simulating intermediate resonances in this decay would produce rich strong phase information arising from the interference between with the intermediate decays. The possible intermediate resonances are tabulated below:

Light Unflavored Mesons ($S = C = B = 0$)

Particle Name	Mass [MeV]	Full width, Γ [MeV]	J^P	Decay Channel
$f_0(980)$	980 ± 10	$40 \rightarrow 100$	0^+	$f_0(980) \rightarrow K\bar{K}$
$a_0(980)$	980 ± 20	$50 \rightarrow 100$	0^+	$a_0(980) \rightarrow K\bar{K}$
$\phi(1020)$	1019.45 ± 0.02	4.26 ± 0.04	1^-	$\phi(1020) \rightarrow K^+K^-$
$b_1(1235)$	1229.5 ± 3.2	142 ± 9	1^+	$b_1(1235) \rightarrow [\phi \rightarrow K^+K^-]\pi$ and $b_1(1235) \rightarrow [K^*(892)^\pm \rightarrow K\pi]K^\pm$
$a_1(1260)$	1230 ± 40	$250 \rightarrow 600$	1^+	$a_1(1260) \rightarrow [f_0(1370) \rightarrow K\bar{K}]\pi$ and $a_1(1260) \rightarrow [f_2(1270) \rightarrow K\bar{K}]\pi$ and $a_1(1260) \rightarrow K[\bar{K}^*(892) \rightarrow K\pi] + c.c.$
$f_2(1270)$	1275.1 ± 1.2	$185.1^{+2.9}_{-2.4}$	2^+	$f_2(1270) \rightarrow K\bar{K}$
$f_1(1285)$	1281.8 ± 0.6	24.3 ± 1.1	1^+	$f_1(1285) \rightarrow K\bar{K}\pi$
$\eta(1295)$	1294 ± 4	55 ± 5	0^-	$\eta(1295) \rightarrow a_0(980)\pi$
$a_2(1320)$	1318.3 ± 0.6	107 ± 5	2^+	$a_2(1320) \rightarrow K\bar{K}$
$f_0(1370)$	$1200 \rightarrow 1500$	$200 \rightarrow 500$	0^+	$f_0(1370) \rightarrow K\bar{K}$
$\eta(1405)$	1409.8 ± 2.5	51.1 ± 3.4	0^-	$\eta(1405) \rightarrow [a_0(980) \rightarrow K\bar{K}]\pi$ and $\eta(1405) \rightarrow K\bar{K}\pi$ and $\eta(1405) \rightarrow K[\bar{K}^*(892) \rightarrow K\pi]K$
$f_1(1420)$	1426.4 ± 0.9	54.9 ± 2.6	1^+	$f_1(1420) \rightarrow K\bar{K}\pi$ and $f_1(1420) \rightarrow K[\bar{K}^*(892) \rightarrow K\pi] + c.c.$
$a_0(1450)$	1474 ± 19	265 ± 13	0^+	$a_0(1450) \rightarrow K\bar{K}$
$\rho(1450)$	1465 ± 13	265 ± 13	0^+	$\rho(1450) \rightarrow K[\bar{K}^*(892) \rightarrow K\pi] + c.c.$
$\eta(1475)$	1476 ± 4	85 ± 9	0^-	$\eta(1475) \rightarrow K\bar{K}\pi$ and $\eta(1475) \rightarrow [a_0(980) \rightarrow K\bar{K}]\pi$ and $\eta(1475) \rightarrow K[\bar{K}^*(892) \rightarrow K\pi] + c.c.$
$f_0(1500)$	1505 ± 6	109 ± 7	0^+	$f_0(1500) \rightarrow K\bar{K}$
$f'_2(1525)$	1525 ± 5	73^{+6}_{-5}	2^+	$f'_2(1525) \rightarrow K\bar{K}$
$\eta_2(1645)$	1617 ± 5	181 ± 11	2^-	$\eta_2(1645) \rightarrow [a_2(1320) \rightarrow K\bar{K}]\pi$ and $\eta_2(1645) \rightarrow K\bar{K}\pi$ and $\eta_2(1645) \rightarrow [K^*(892) \rightarrow K\pi]\bar{K}$ and $\eta_2(1645) \rightarrow [a_0(980) \rightarrow K\bar{K}]\pi$
$\pi_2(1670)$	1672.2 ± 3.0	260 ± 9	2^-	$\pi_2(1670) \rightarrow [f_2(1270) \rightarrow K\bar{K}]\pi$ and $\pi_2(1670) \rightarrow K[\bar{K}^*(892) \rightarrow K\pi] + c.c.$
$\phi(1680)$	1680 ± 20	150 ± 50	1^-	$\phi(1680) \rightarrow K\bar{K}$ and $\phi(1680) \rightarrow K[\bar{K}^*(892) \rightarrow K\pi] + c.c.$
$\rho_3(1690)$	1688.8 ± 2.1	161 ± 10	3^-	$\rho_3(1690) \rightarrow K\bar{K}\pi$ and $\rho_3(1690) \rightarrow K\bar{K}$ and $\rho_3(1690) \rightarrow [a_2(1320) \rightarrow K\bar{K}]\pi$
$\rho(1700)$	1720 ± 20 ($\eta\rho^0$ & $\pi^+\pi^-$)	250 ± 100 ($\eta\rho^0$ & $\pi^+\pi^-$)	1^-	$\rho(1700) \rightarrow K\bar{K}$ and $\rho(1700) \rightarrow K[\bar{K}^*(892) \rightarrow K\pi] + c.c.$
$f_0(1710)$	1720 ± 6	135 ± 8	0^+	$f_0(1710) \rightarrow K\bar{K}$
$\pi(1800)$	1812 ± 12	208 ± 12	0^-	$\pi(1800) \rightarrow [K^*(892) \rightarrow K\pi]\bar{K}^-$
$\phi_3(1850)$	1854 ± 7	87^{+28}_{-23}	3^-	$\phi_3(1850) \rightarrow K\bar{K}$ and $\phi_3(1850) \rightarrow K[\bar{K}^*(892) \rightarrow K\pi] + c.c.$
$f_2(1950)$	1944 ± 12	472 ± 18	2^+	$f_2(1950) \rightarrow K\bar{K}$
$f_2(2010)$	2011^{+60}_{-80}	202 ± 60	2^+	$f_2(2010) \rightarrow K\bar{K}$
$a_4(2040)$	1996^{+10}_{-9}	255^{+28}_{-24}	4^+	$a_4(2040) \rightarrow K\bar{K}$ and $a_4(2040) \rightarrow [f_2(1270) \rightarrow K\bar{K}]\pi$
$f_4(2050)$	2018 ± 11	237 ± 18	4^+	$f_4(2050) \rightarrow K\bar{K}$ and $f_4(2050) \rightarrow [a_2(1320) \rightarrow K\bar{K}]\pi$
$f_2(2300)$	2297 ± 28	149 ± 40	2^+	$f_2(2300) \rightarrow K\bar{K}$

Table 1: Table of possible resonances for the light unflavored mesons.

Strange Mesons ($S = \pm 1, C = B = 0$)

Particle Name	Mass [MeV]	Full width, Γ [MeV]	J^P	Decay Channel
$K^*(892)$	895.5 ± 0.8	46.2 ± 1.3	1^-	$K^*(892) \rightarrow K\pi$
$K^*(892)^\pm$	891.66 ± 0.26	50.8 ± 0.9	1^-	
$K^*(892)^0$	895.94 ± 0.22	48.7 ± 0.8	1^-	
$K_1(1270)$	1272 ± 7	90 ± 20	1^+	$K_1(1270) \rightarrow K[f_0(1370) \rightarrow K\bar{K}]$
$K_1(1400)$	1403 ± 7	174 ± 13	1^+	$K_1(1400) \rightarrow K[f_0(1370) \rightarrow K\bar{K}]$
$K^*(1410)$	1414 ± 15	232 ± 21	1^-	$K^*(1410) \rightarrow K\pi$
$K_0^*(1430)$	1425 ± 50	270 ± 80	0^+	$K_0^*(1430) \rightarrow K\pi$
$K_2^*(1430)^\pm$	1425.6 ± 1.5	98.5 ± 2.7	2^+	$K_2^*(1430) \rightarrow K\pi$
$K_2^*(1430)^0$	1432.4 ± 1.3	109 ± 5	2^+	
$K^*(1680)$	1717 ± 27	322 ± 110	1^-	$K^*(1680) \rightarrow K\pi$
$K_2(1770)$	1773 ± 8	186 ± 14	2^-	$K_2(1770) \rightarrow K[f_2(1270 \rightarrow K\bar{K}) \text{ and } K_2(1770) \rightarrow K[\phi \rightarrow K^+K^-]]$
$K_3^*(1780)$	1776 ± 7	159 ± 21	3^-	$K_3^*(1780) \rightarrow K\pi$
$K_2(1820)$	1816 ± 13	276 ± 35	2^-	$K_2(1820) \rightarrow K[f_2(1270) \rightarrow K\bar{K}]$
$K_4^*(2045)$	1045 ± 9	198 ± 30	4^+	$K_4^*(2045) \rightarrow K\pi$

Table 2: Table of possible resonances for the strange mesons.

4 Decay Angles

4.1 $\psi(3770) \rightarrow D^0\bar{D}^0$ decay

In the next section we are interested in examining the distribution of the decay angle between product pairs in various simulated decays. By examining the distribution of decay angles in the laboratory frame this angle can be used to distinguish the background (which should not have a strongly peaked angle dependence) from the decays in which we are interested. This is due to the ultra-relativistic parent particle beaming the decay products in the direction of movement, while the background should not follow such a strongly beamed angle distribution.

The decay angles were obtained by relativistically boosting the MC simulated Lorentz vectors using the `Boost()::TLorentzVector` method. The `TVector3` vectors used to boost the parent particles were obtained from fits to the momentum component distributions of previously calculated LHCb MC simulation data. The `GetRandom()::TF1` method was then used to provide a random distribution following that of the LHCb MC data. The boost was repeated a large number (10^6) of times, each time boosted by a different 3-vector provided by the random momentum distribution following the LHCb MC data, and each time the angle between the resulting particles was calculated and plotted to provide final angle distribution functions in the lab frame. This angle distribution can then be used to distinguish these vital decays from the background, provided it is sharply peaked enough.

The first decay for which this was done was the $\psi(3770) \rightarrow D^0\bar{D}^0$ decay.

Before the LHCb MC momentum component distribution data could individually be used to provide 3-vectors to boost the $\psi(3770)$, it had to be established that there was no correspondence or correlation between the individual momentum components. Table 3 shows the calculated correlation factors between the individual direction components, whilst Figure 5 visualises the dependence of the components on one another. Both clearly show no correlation between individual momentum components. Thus, they can be considered independent distributions and the random component generation can be done separately.

	p_x	p_y	p_z
p_x	1	0.00640212	0.0150375
p_y	0.00640212	1	0.0167604
p_z	0.0150375	0.0167604	1

Table 3: The correlation factors between each momentum component. Note that these are all extremely low, thus the components can be considered independent of one another.

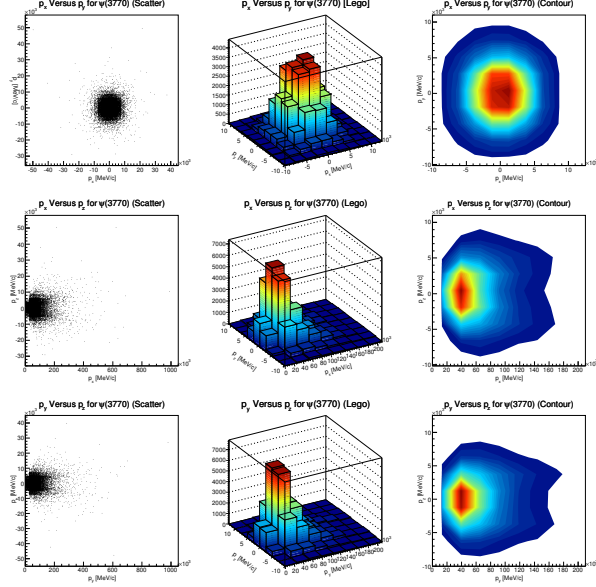


Figure 5: Different visualisations of the correlation between different momentum components in the LHCb MC data. These clearly show no correlation. Note that the $x - z$ and $y - z$ plots are skewed to the right as z is always positive.

The x and y components of the momentum were fitted to Gaussian distributions, whilst the z component of the momentum was fitted to a Landau up until 62 GeV/, after which it was fitted to a Gaussian, as shown in Figure 6. Note that the fits are not perfect, but follow the general distribution satisfactorily for the purposes of our random momentum generation.

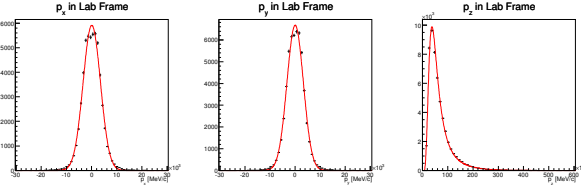


Figure 6: Fits to the momentum component distributions. ROOT’s `GetRandom()::TF1` method was then used to provide a random distribution based on these fits.

The final decay angle distribution between the D^0 and \bar{D}^0 is shown in Figure 7. Note that all decay angles are $< 5^\circ$, with a high peak at around $\sim 0.5^\circ$, meaning that the decay angle can be used to separate the $\psi(3770)$ decays from the background.

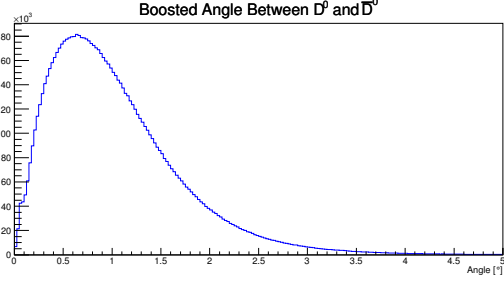


Figure 7: The final lab frame decay angle distribution between D^0 and \bar{D}^0 . Note that the distribution is sharply peaked about $\sim 5^\circ$, with no angles $> 5^\circ$.

4.2 $B \rightarrow (\psi(3770) \rightarrow D^0 \bar{D}^0)K$ decay

As with the $\psi(3770)$ decay, LHCb MC momentum data was used to provide a distribution to use for the Lorentz boost. However, only $B \rightarrow D$ Bach (where the bachelor particle is either a kaon or a pion) momentum data was available. Hence conservation of momentum was used to determine the parent B momentum from the D and bachelor particle momenta.

The corresponding correlation factor table is shown below in Table 4, while the correlation visualisations are shown in Figure 8:

	p_x	p_y	p_z
p_x	1	0.0165178	-0.00486466
p_y	0.0165178	1	0.017408
p_z	-0.00486466	0.017408	1

Table 4: The correlation factors of the momentum components of the B meson, obtained from LHCb $B \rightarrow D$ Bach MC data.

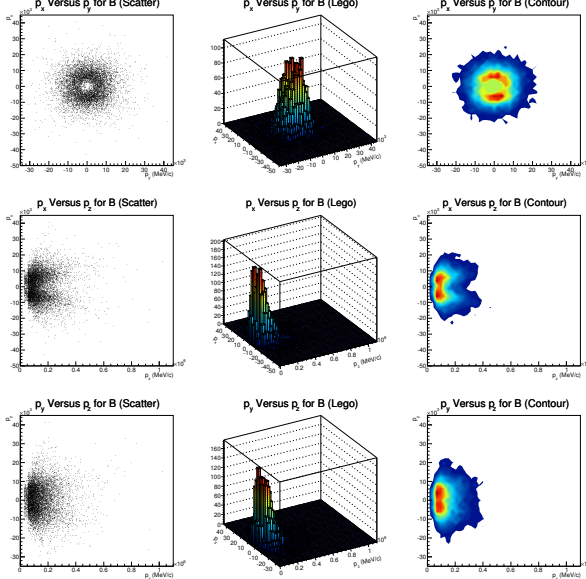


Figure 8: Visualisations of the correlation between momentum components of the B meson, obtained from $B \rightarrow D$ *Bach* LHCb MC data. Note the hole present in the $x - y$ graphs.

The momentum components were once again fitted to mathematical functions, again a Gaussian for x and y components and for the z component a Landau up until $130\text{ GeV}/\zeta$, after which a Gaussian. Note that the x and to a lesser extent the y component distributions cut off at low values. This is most likely due to specific detector design and is thus ignored for the purposes of the mathematical fit, which intends only to find the general distribution of B meson momentum components. The resulting fits are illustrated in Figure 9.

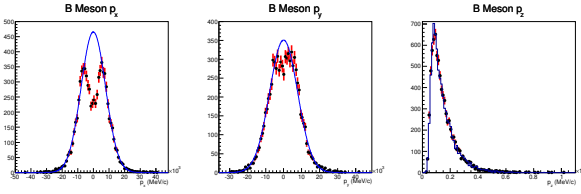


Figure 9: The momentum component distributions for the B meson, along with their mathematical fits. Note the gap in the x and y component distributions near the 0 point.

The angle distributions between the $\psi(3770)$ and K and between the D^0 and \bar{D}^0 product particles was then plotted both in the rest frame of the parent B meson and in the lab frame, i.e. the Lorentz boosted frame. The plots are shown below in Figures ??:

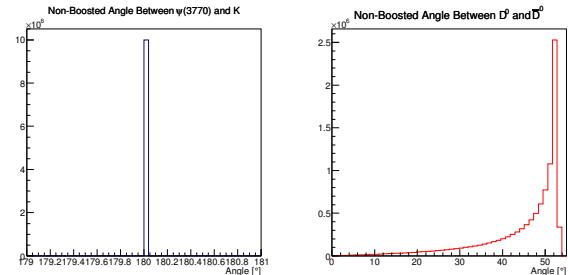


Figure 10: The decay angle distributions in the rest frame of the parent B meson. Note the sharp cut off at $\sim 50^\circ$ for the $D^0-\bar{D}^0$ decay angle distribution.

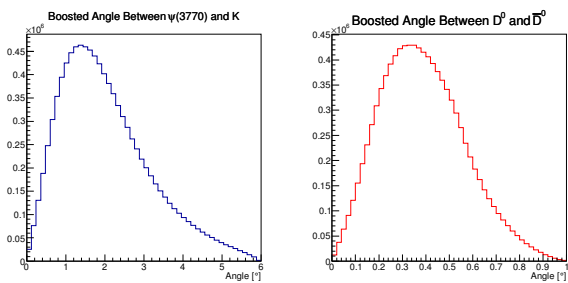


Figure 11: The decay angle distributions in the lab frame. Note that both distributions are contained within a small range of angles, $\lesssim 6^\circ$ for the $\psi(3770)-K$ angle and $\lesssim 1^\circ$ for the $D^0-\bar{D}^0$ angle.

Both of these distributions are contained in a small range of angles and are sharply peaked, with the $\psi(3770)-K$ angle at around $\simeq 1.5^\circ$, and the $D^0-\bar{D}^0$ angle at around $\simeq 0.4^\circ$. This confirms that $B \rightarrow (\psi(3770) \rightarrow D^0 \bar{D}^0)K$ decays can be easily distinguished from the background due to the sharp angular peaking in the $\psi(3770) \rightarrow D^0 \bar{D}^0$ product decay, allowing for its use in isolating $\psi(3770)$ decays for the study of symmetry violation.

References

- [1] J. Beringer et al. “Review of Particle Physics”. In: *Phys. Rev. D* 86 (1 July 2012), p. 010001. doi: [10.1103/PhysRevD.86.010001](https://doi.org/10.1103/PhysRevD.86.010001). URL: <http://link.aps.org/doi/10.1103/PhysRevD.86.010001>.